A Simple and Efficient Visible Light Photodetector based on Co3O4/ZnO Composite

Aneela Tahira
Linkopings universitet
Raffaello Mazzaro
Università di Bologna: Universita di Bologna
Federica Rigoni
Lulea University of Technology: Lulea Tekniska Universitet
Ayman Nafady
King Saud University
Shoyebmohamad F Shaikh
King Saud University
Asma A. Al-Othman
King Saud University
Razan A. Alshgari
King Saud University
Zafar Hussain Ibupoto (zaffar.ibhupoto@usindh.edu.pk)
University of sindh Jamshoro https://orcid.org/0000-0002-6756-9862

Research Article

Keywords: ZnO nanorods, Co3O4 nanosheets, heterojunction, visible light photodetector

Posted Date: June 11th, 2021

DOI: https://doi.org/10.21203/rs.3.rs-530646/v1

Abstract

Herein, we propose for the first time visible light photodetector based on n-type ZnO nanorods decorated with p-type Co_3O_4 nanowires. The heterojunction was fabricated on fluorine doped tin oxide (FTO) glass substrate by low temperature aqueous chemical growth method. ZnO exhibits nanorod morphology and cobalt oxide possesses nanowire shape with sharp tail. Energy dispersive spectroscopy (EDS) confirmed the presence of Zn, O, and Co elements in the heterojunction. ZnO and Co_3O_4 have hexagonal and cubic phases, respectively, as confirmed by XRD. The dense and perpendicular ZnO nanorods are acting as a scattering layer for visible light, while Co_3O_4 nanowires act as a visible-light absorber. The all oxide p-n junction can operate as visible light photodetector. Furthermore, the heterojunction also shows a reproducible and fast response for the detection of visible light. Optimization of the device is needed (presence of buffer layers, tuning a thickness of the optical absorber) to improve its functionalities.

1. Introduction

The development of new architectures and materials combination for optoelectronic devices, like photodetectors, is boosting the research in the field. The main target is the development of low-cost processes to produce highly efficient and stable devices not containing harmful or expensive materials. An extended range of heterostructures for the photo detection application have been reported [1] like $BiOCl/TiO_2$ [2], grapheme/GaAs [3], SnO_2/NiO [4], $SrTiO_3$/CuS-ZnS [5], ZnO/NiO [6], Ag-doped ZnO [7], ZnO/Ga_2O_3 [8].

It is worth to note mention here that these devices are limited by slow photo response ranging from millisecond to seconds and short wavelength sensing. Thus, it is highly desirable to sense the wide spectral range with swift switching response for the photodetector by using photosensitive compounds. The materials of earth abundant and nontoxicity are highly critical for the large scale application and mass production of devices in diverse ongoing research fields. The metal oxides of wide bandgap are found very potential materials for the design of efficient photodetector geometries. Among them, zinc oxide (ZnO) is n-type, wide band gap (~3.37eV), emiconducting metal oxide, nontoxic and earth abundant in nature has been capitalized as active UV light absorber and used in in different highly sensitive photodetectors [9]. For making the p-n junction with ZnO, the large utilization of p-type metal oxides are (NiO), cuprous oxide (Cu_2O), spinel cobalt oxide (Co_3O_4) and so on [10–13].

Cobalt oxide (Co_3O_4) has been highly investigated in various applications such as gas sensing [14], supercapacitors [15], Lithium ion batteries, [16] and in solar cells [17]. Like Cu_2O, Co_3O_4 is a p-type, earth abundant, non-toxic, semiconducting material. Its absorption spectrum is characterized by two direct transitions in the visible spectral range, corresponding to optical bandgaps of 1.5 eV and 2.2 eV [18, 14]. Thanks to the low bandgap, and the possibility to further optimize it. Generally it is believed that the Co_3O_4 exhibits spinel structure with mixed valence states. The Co_3O_4 being a p-type it is allowing the acceptor states which accelerates the trapping of charge thus it creates the charge transport. Because of

the dual and indirect bandgaps of Co_3O_4 2.2 eV and 1.6 eV and it in spinel structure it contains Co3p and Co 2p spin states. It is a common observation that the dual bandgaps lead to the design of efficient photodetectors [19, 20]. These unique features of ZnO and Co_3O_4 altogether share the development of wide spectral photodetectors. The Co_3O_4 nanostructures have been produced through different methods like solution, spray pyrolysis, and chemical vapor deposition [21–24].

The p-n junction of ZnO-Co_3O_4 can be applied as efficient photodetector. A photosensor is a device, which generates photocurrent as a response to light. A photodiode is a device that converts light into electric current, commonly termed as photodetector, light detector or photosensor. Photodiodes typically work in reverse bias; the efficiency of these devices is mainly depending on the high surface charge carrier concentration [25]. Thus, in order to maximize the photo response, different kind of heterostructures were investigated, to exploit increased light absorption due to multiple scattering, and to increase the interface area, and maximize exciton dissociation rate at the interface [26–32]. Moreover, there are numerous heterostructures both inorganic and inorganic-organic photodetectors, which employ transparent n-type semiconducting metal oxides including ZnO because of its capability to absorb UV light efficiently [33–36]. Beside this, Co_3O_4 as p-type metal oxide can be a good light absorber for visible photodetectors due to its direct optical transitions in the visible range.

It is the simplicity, cost, processing nature and energy consumption during a growth method which are keep in mind for the mass production of nanostructured materials. For this purpose, there is no report about the p-n junction of Co_3O_4/ZnO using low temperature aqueous chemical growth method for the development of visible light photodetector.

In this work, we investigated for the first time the system composed of hydrothermally grown ZnO nanorods covered by Co_3O_4 nanowires on fluorine doped tin oxide (FTO) glass, to be applied as photodetector. At the same time, the all oxide p-n junction can act as visible-light photodetector with fast response and good stability.

2. Experimental Section

2.1. Chemicals

Zinc acetate di-hydrate, methanol 99%, ethanol 99.5 %, potassium hydroxide, hexamethylenetetramine, cobalt chloride hexahydrate, urea, polyethylene glycol was purchased from Sigma-Aldrich. All the other chemicals used were of analytical grade. All the solutions were prepared in the distilled water.

2.2. Synthesis of ZnO/Co_3O_4 heterojunctions

ZnO nanorods were fabricated on FTO glass substrate. First, a seed layer of ZnO nanoparticles was deposited on cleaned FTO substrate and annealed at 130 °C for 20 minutes. Annealing ensures the firm binding of ZnO seed particles on the substrate. The seed solution was prepared by mixing 0.274 g of zinc

acetate di-hydrate in 125 mL of methanol and 0.109 g of KOH dissolved in 65 mL of methanol that was prepared separately. Then KOH solution was mixed dropwise in zinc acetate di-hydrate solution at constant stirring and temperature of 60 °C for 2 hours. The growth solution was prepared by using equimolar concentration of 50 mM of zinc nitrate hexahydrate and hexamethylenetetramine in the presence of 100 mg of polyethylene glycol as soft template in 100 mL of distilled water. The seed layer coated FTO substrates were immersed in a beaker containing the growth solution, with the conducting side facing downwards. The beaker containing the growth solution was covered with aluminum foil tightly. Then the growth solution was kept in preheated electric oven for 4.5 hours at 95 °C. After the completion of the growth process, the substrates were gently washed with distilled water to remove the residual particles and dried at room temperature. Co_3O_4 nanostructures were prepared on the top of ZnO nanorods to obtain the composite heterostructures. ZnO nanorods were covered with seed particles of cobalt (prepared by mixing 0.68 grams in 30 mL methanol and 0.1 gram of KOH) and annealed at 130 °C for 20 min. A 0.1M solution of cobalt chloride hexahydrate and urea in 100 mL of water was prepared, containing 0.1 gram of polyethylene glycol as templating agent. The ZnO nanorods coated with cobalt oxide seed particles were dipped in the growth solution. The growth solution was covered by aluminum foil and left in preheated electric oven for 4.5 hours at 95 °C. After the completion of the growth process, the samples were taken out from the beaker, washed with the distilled water, and dried at room temperature. Afterwards, cobalt hydroxide nanostructures were converted into Co_3O_4 by annealing in muffle furnace for 3 hours at 500 °C in air. Additionally, pristine Co_3O_4 nanostructures were prepared by the same method using equimolar 0.1M concentration of cobalt chloride hexahydrate and urea at 95 °C for 4.5 hours and consequently the obtained cobalt hydroxide phase was converted into oxide phase by annealing sample at 500 °C for 3 hours in air. The samples were characterized by SEM (FEI Magellan™ HR-SEM) and XRD (Empyrean instrument, PANalytical PIXcel^{3D}, with Cu Kα X-ray source, Bragg Brentano geometry) techniques. PV measurements were carried out at the illumination of air mass 1.5 global (AM 1.5G) using a solar simulator calibrated with a silicon calibrated solar cell. We used thermally evaporated circular gold back contacts, 55 nm thick and 2 mm in diameter. In addition, small portion of the deposited material on the FTO substrate was chemically etched and removed to access bare FTO for front contact. Similar method was used for making gold contacts on pure ZnO and cobalt oxide. The I-V characteristics of visible photodetector was measured by Solartron Analytical ModuLab XM multi-purpose potentiostat, using cyclic voltammetry at the bias voltage of -1 to 1 V, either in dark or under illumination with an air mass 1.5 global (AM 1.5G) calibrate solar simulator. The photo response was recorded at + 1 V under chopped illumination. The transmittance and diffused reflectance for the various nanostructures were measured via Agilent UV-Visible spectrophotometer at room temperature in transmission mode and using an integrating sphere, respectively.

3. Results And Discussion

Figure 1 shows the fabrication process of all oxide heterojunctions composed of ZnO nanorods decorated with Co_3O_4 nanowires. Uniform, well aligned and dense ZnO nanorods grow perpendicular to the FTO substrate exhibiting hexagonal facets and were then covered with Co_3O_4 nanowires (Fig. 1).

Figure 2 shows the cross-section image of pure ZnO, pure Co_3O_4 and the heterojunction based on Co_3O_4 nanowires over the ZnO nanorods. ZnO nanorods are completely covered by grass-like nanowire structure of Co_3O_4. The surface of ZnO nanorods is etched during the deposition of Co3O4 due to the use of cobalt chloride where chloride ion etched the top surface of ZnO. The thickness of the ZnO layer is around 580 nm and the thickness of the compact Co_3O_4 layer is about 500 to 700 nm. Some overgrown Co_3O_4 nanowires, a few microns in length, are visible in the cross-section image. The elemental distribution along the cross-section of the composite system indicates the presence of Zn, O, Co and Sn at the expected position. The EDS analysis revealed the homogeneous distribution of each element in the respective part of the heterojunction, suggesting that the ZnO underlying layer is maintained during the Co_3O_4 growth as shown in Fig. 2. Figure 3 is reporting the XRD analysis of the ZnO/Co_3O_4 sample and the comparison the single components grown on FTO substrates. The XRD pattern of pure ZnO (Fig. 3b) exhibits the typical ZnO hexagonal crystal phase and the diffraction peaks are in good agreement with the standard JCPDS card no. 96-00-4182, in addition to some peaks coming from the FTO substrate (Fig. 3a as reference). The intense (002) peak is suggesting a c-axis oriented growth of ZnO nanorods, as previously reported [37]. XRD confirms the cubic phase of the Co_3O_4 structures, according to the standard JCPDS card no. 96-900-5889 as shown in Fig. 3 (c). The XRD pattern of the composite (Fig. 3(d)) indicates the presence of both hexagonal phase from ZnO and cubic phase from Co_3O_4, as expected. No spurious phases are detected in the sample, in good agreement with elemental composition obtained from EDS analysis.

UV-Visible transmittance spectrum and diffused reflectance of ZnO, Co_3O_4 and ZnO/Co_3O_4 structures are reported in Fig. 4 (a.b). ZnO sample is showing the typical band edge related drop in transmittance and reflectance below 375 nm. For pristine cobalt oxide, a wide absorption band ranging from 300 nm to 550 nm is noticeable in transmission spectrum, with a second peak centered at 720 nm, consistent with the double band-gap energy characterizing Co_3O_4. [38] The composite nanostructures exhibit strong absorption above 500 nm due to the thick Co_3O_4 layer. As the SEM results have proved, the Co_3O_4 top layer has also a NW structure, which can enhance light scattering. Since Co_3O_4 is a low bandgap semiconductor the trapped photons will be preferentially absorbed, rather than diffused, as in the case of ZnO." Such UV-Visible characteristics for Co_3O_4 and its composite agree with results in the literature [39].

In diffuse reflectance spectra (Fig. 4 (b), the highest intensity in the visible region is observed in ZnO nanorods, while it is drastically decreased for the composite and pure cobalt oxide nanostructures, due to strong light absorption from Co_3O_4. This is a promising result in terms of Sun light absorption from the composite heterostructures.

Figure 5(a) shows the response of visible light photodetector based on Co_3O_4/ZnO p-n junction in the dark and under simulated Sunlight. The current voltage (I-V) response shows the typical behavior of a p-n junction, with the current increasing with the applied voltage in dark. A drastic increase of the steepness of the I-V curve is recorded under illumination, indicating that a strong decrease of the device resistance is taking place, since the light absorption is producing an increase of the number of carriers due to the

exciton generation and separation, and charge collection at the two electrodes. Importantly, high intensity of light and voltage can push faster photo-generated charge carriers towards the electrodes and minimizing the recombination of hole-electron pairs [40, 41]. Figure 5(b) shows the dependence of the current on time under on/off light for each interval of 20 s. The rise in photocurrent is significant (in the ms regime) and become reasonably stable under illumination, while slowly decaying to the original current value. The slow decay of the OFF cycle suggests a low recombination rate of the generated charges, probably due to the limited conductivity of the Co_3O_4 layer. However, the photocurrent generated largely exceeds the limited increase in the baseline current observed in dark condition, in contrast to what happens in the pure ZnO sample (Fig. 6 (c, d)). The repeatability and the large ON-OFF photocurrent ratio for this Co_3O_4/ZnO heterojunction suggest promising application as visible light photodetector.

4. Conclusions

In summary, a simple methodology is used for the first time for the fabrication of heterostructure based on Co_3O_4 nanowires decorated on ZnO nanorods by hydrothermal method. ZnO nanorods are completely covered by thick layer of Co_3O_4 nanowires, which is confirmed by the topographical and cross section SEM images. The ZnO layer exhibits a thickness of 580 nm, whereas compact Co_3O_4 layer has thickness of 500 to 700 nm. Both EDS and XRD studies are in good agreement by giving a definite information about the composition of heterostructures, which is comprised, on the Co_3O_4 and ZnO nanomaterials. The junction exhibits interesting features in terms of light responsivity rate and reliability, which suggest the application as visible light photodetector. Thanks to the extremely trivial and scalable synthetic approach, the presented ZnO/Co_3O_4 is appealing for low power/low price photodetectors that can be employed in portable and wearable devices.

Declarations

Acknowledgment

A. N, S.F.S, A. A. A, and R. A. A extend their sincere appreciation to the Deanship of the Scientific Research at King Saud University for funding this project through Research Group (RG #236)

References

1. Chen, C., Ouyang, W., Yang, W., Fang, X.: Recent Progress of Heterojunction Ultraviolet Photodetectors: Materials, Integrations, and Applications. Adv. Funct. Mater. **30**, 1909–1923 (2020)
2. Ouyang, W., Teng, F., Fang, X.: High Performance BiOCl Nanosheets/TiO2 Nanotube Arrays Heterojunction UV Photodetector: The Influences of Self-Induced Inner Electric Fields in the BiOCl. Nanosheets.Adv. Funct. Mater. **28**, 1707–1720 (2018)
3. Tao, Z., Zhou, D., Yin, H., Cai, B., Huo, T., Su, Y.: A facile method for preparation of emulsion using the high gravity technique.Mater. Sci. Semicond. Process. **111**, 1049–1058 (2020)

4. Long, Z., Xu, X., Yang, W., Hu, M., Shtansky, D., Golberg, D., Fang, F.: Monolayer Doping: A Shallow Acceptor of Phosphorous Doped in MoSe2 Monolayer Adv. Electron. Mater **6**, 1901–1912 (2020)
5. Zhang, Y., Xu, X., Fang, X.: Tunable self-powered n-SrTiO3 photodetectors based on varying CuS-ZnS nanocomposite film (p-CuZnS, p-CuS, and n-ZnS). InfoMat **1**, 542–551 (2019)
6. Zhang, Z., Ning, Y., Fang, X.: From nanofibers to ordered ZnO/NiO heterojunction arrays for self-powered and transparent UV photodetectors. J. Mater. Chem. C. **7**, 223–229 (2019)
7. Ning, Y., Zhang, Z., Teng, F., Fang, X.: Role of Surface RGD Patterns on Protein Nanocages in Tumor Targeting Revealed Using Precise Discrete Models. Small. **14**, 1703–1712 (2018)
8. Zhao, B., Wang, F.,Chen,H., Zheng, L., Su, L., Zhao, D., Fang, F.: TpyCo2+-Based Coordination Polymers by Water-Induced Gelling Trigged Efficient Oxygen Evolution Reaction. Adv. Funct. Mater. **27**, 1700–1711 (2017)
9. Ferhati, H., Djeffal, F., Benhaya, A.: Structural and electrical properties of Ba-substituted spinel ferrites.Mater. Sci. Semicond. Process. **119**, 1049–1056 (2020)
10. Kumar, M., Patel, M., Kim, J., Kim, B.: Chemical epitaxy of π-phase cubic tin monosulphide. Mater. Lett **13**, 122–125 (2018)
11. Zhang, D., Gu, X., Jing, F., Gao, F., Zhou, J., Ruan, S.: Studies on the Influence of Growth Time on the Rutile TiO2 Nanostructures Prepared on Si Substrates with Fabricated High-Sensitivity and Fast-Response p-n Heterojunction Photodiode. J. Alloys Compd. **618**, 551–554 (2015)
12. Chen, H., Liu, K., Hu, L., Ghamdi, A., Fang, X.: Ultraviolet Detectors Based on Wide Bandgap Semiconductor Nanowire: A Review. Mater. Today **18**, 493–502 (2015)
13. Klochko, N.P., et al.: Structure and properties of nanostructured ZnO arrays and ZnO/Ag nanocomposites fabricated by pulsed electrodeposition. Sol. Energy **164**, 149–159 (2018)
14. Fu, Q.M., et al.: Tin-doped comb-like CdS microstructure and construction of the micro-sliding rheostat. Mater. Lett. **222**, 74–77 (2018)
15. Rana, A.K., Park, J., Kim, J., Wong, C.: Nano energy for miniaturized systems. Nano Energy **64**, 1039–1041 (2019)
16. Nam, H., Sasaki, T., Koshizaki, N.:Thickness and Morphology Effects on Optical Gas-Sensing Response Using Nanostructured Cobalt Oxide Films Prepared by Pulsed Laser Ablation. *J. Phys. Chem.B. 110,110 – 21 (2006)*
17. Patil, P., Kadam, L., Lokhande, C.: Preparation and characterization of spray pyrolysed cobalt oxide thin films. Thin Solid Films. **272**, 29–39 (1996)
18. Barreca, D., Massignan, C.: Composition and Microstructure of Cobalt Oxide Thin Films Obtained from a Novel Cobalt(II) Precursor by Chemical Vapor Deposition. Chem. Mater. **13**, 588–599 (2001)
19. Kandalkar, S., Gunjakar, J., Lokhande, C.: Preparation of cobalt oxide thin films and its use in supercapacitor application. Appl. Surf. Sci. **254**, 5540–5549 (2018)
20. Chen, C., Buysman, A., Kelder, E.: Schoonman, J.: Electrostatic spray deposition of thin layers of cathode materials for lithium battery. Solid State Ionics. **80**, 1261–1282 (1995)

21. Ghamgosar, P., et al.: Self-Powered Photodetectors Based on Core-Shell ZnO-Co3O4 Nanowire Heterojunctions. ACS Appl. Mater. Interfaces **11**, 23454–23462 (2019)
22. Kandalkar, S., Gunjakar, J., Lokhande, C.: Study of structural and electronic environments of hydrogenated amorphous silicon carbonitride (a-SiCN:H) films deposited by hot wire chemical vapor deposition. Appl. Surf. Sci. **254**, 5540–5540 (2008)
23. Qiao, C., et al.: Nature of the band gap and origin of the electro-/photo-activity of Co3O4.J. Mater. Chem. C **1**, 4628–4633 (2013)
24. Cheng, C., Serizawa, M., Sakata, H., Hirayama, T.: Electrical conductivity of Co3O4 films prepared by chemical vapour deposition. Mater. Chem. Phys **53**, 225–230 (1998)
25. Zou, X., Su, J., Silva, R.: Efficient oxygen evolution reaction catalyzed by low-density Ni-doped Co3O4 nanomaterials derived from metal-embedded graphitic C3N4. Chem. Commun. **49**, 7522–7524 (2013)
26. Jiao, F., Frei, H.: Nanostructured cobalt and manganese oxideclusters as efficient wateroxidationcatalysts. Energy Environ. Sci. **3**, 1018–1027 (2006)
27. Nam, H., Sasaki, T., Koshizaki, N.: Structure and Stability of Silver Nanoparticles in Aqueous Solution Produced by Laser Ablation.J. Phys. Chem.B. 110,253 – 62 (2006)
28. Patil, P., Kadam, L., Lokhande, C.: Preparation and Characterization of Sprayed Cobalt Oxide Thin Films.Thin Solid Films. 29,272 – 81 91996)
29. Barreca, D., Massignan, C.: Composition and Microstructure of Cobalt Oxide Thin Films Obtained from a Novel Cobalt(II) Precursor by Chemical Vapor Deposition. Chem. Mater. **13**, 588–596 (2001)
30. Kandalkar, S., Gunjakar, J., Lokhande, C.: Preparation of cobalt oxide thin films and its use in supercapacitor application. Appl. Surf. Sci. **254**, 5540–5553 (2008)
31. Chen, C., Buysman, A., Kelder, E., Schoonman, J.: Solid State Ionics Special Issues. Solid State Ionics **13**, 80–91 (1995)
32. Wu, W., Ting, J., Chang, C.: Zinc(ii) coordination polymers with substituted benzenedicarboxylate and tripodal imidazole ligands: syntheses, structures and properties.CrystEngComm. *12*, 1433–42 (2010)
33. Green.M.: Solar cell efficiency tables.Prog photovoltic Res Appl, 9,123 – 35 (2001)
34. Rana, A.,K., Patel, M., Nguyen, T., Yun, T., Kim, J.-H.: Jo., Mater. Sci. Semicond. Process. **117**, 105192 (2020)
35. Mahala, P., Patel, M., Ban, D.-K., Nguyen, T.,T., Yi, J., Kim, J.: Journal of Alloys and Compound. **827**, 154376 (2020)
36. Veeralingam, S., Yadav, P., Badhulika, S.: Nanoscale. **12**, 9152–9161 (2020)
37. Khun, K., Ibupoto, Z., AlSalhi, M., Atif, M., Ansari, A., Willander, M.: Fabrication of Well-Aligned ZnO Nanorods Using a Composite Seed Layer of ZnO Nanoparticles and Chitosan Polymer. Materials **6**, 4361–4373 (2013)
38. Chen, J., Wu, X., Selloni, A.: Electronic structure and bonding properties of cobalt oxide in the spinel structure. Phys. Rev. B **83**, 2452–2465 (2011)

39. Jana, T., Pal, A., Chatterjee, K.: Photoluminescent Properties of ZrO2: Tm3+, Tb3+, Eu3 + Powders—A.Combined Experimental and Theoretical Study.J. Alloys Compd. 653 – 64: (2015)
40. Xia, J., Zhu, D., Li, X., Wang, L., Tian, L., Li, J., Huang, X.: Meng.X.: Highly sensitive photodetectors based on hybrid 2D-0D SnS2-copper indium sulfide quantum dots.Adv. Funct. Mater. **26**, 4673–4684 (2016)
41. Fu, Y., Gou, G., Wang, X., Chen, Y., Wan, Q., Sun, J., Xiao, S., Huang, H.: Dai.G.: Pressure Effects on Structure and Optical Properties in Cesium Lead Bromide Perovskite Nanocrystals. Appl. Phys. A Mater. Sci. Process. **22**, 123–132 (2017)

Figures

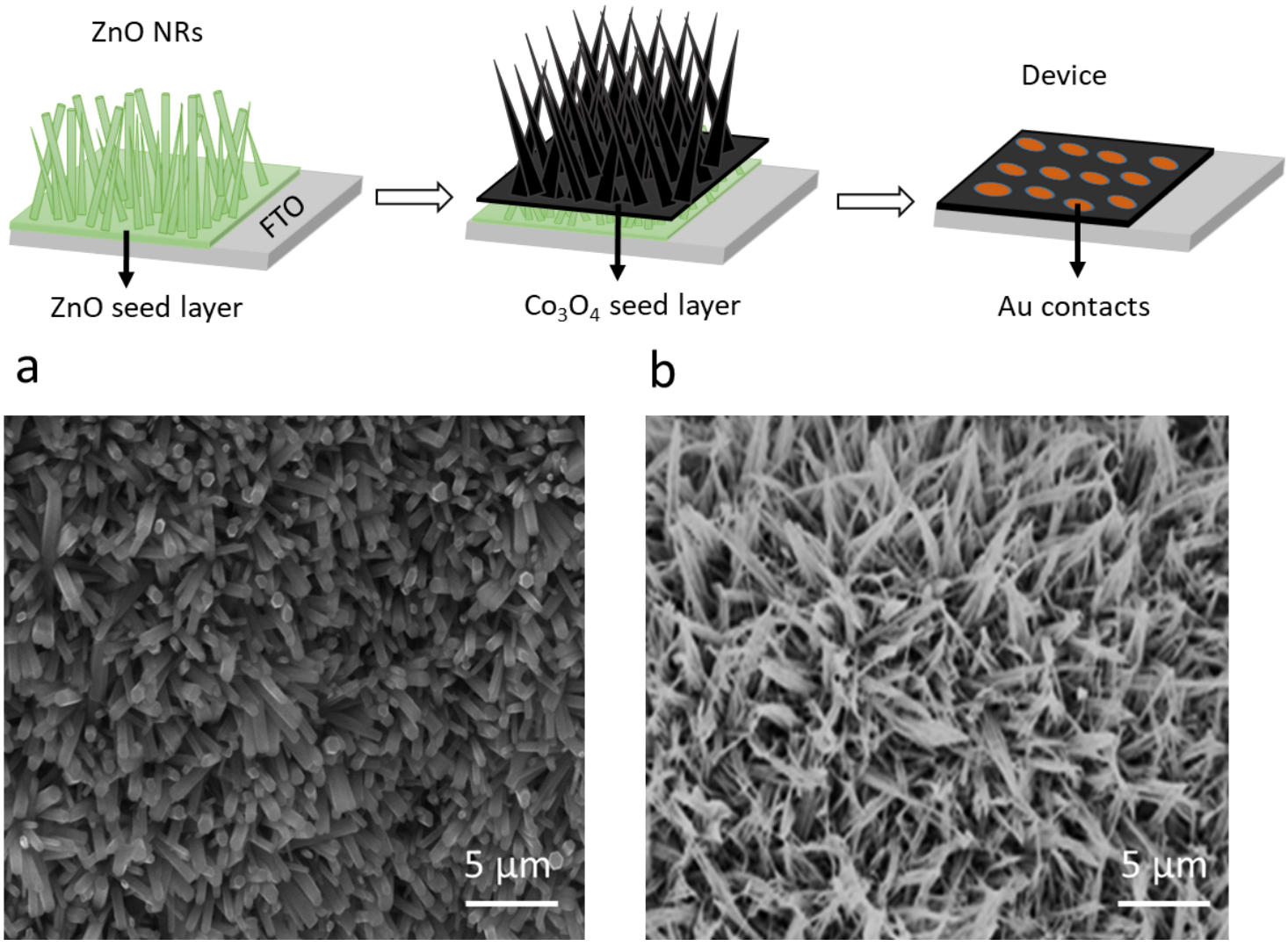

Figure 1

A schematic diagram is describing the fabrication process of photovoltaic device based on Co3O4 deposited on ZnO nanorods (a) SEM image for pure ZnO nanorods, (b). Co3O4/ZnO nanorods SEM images

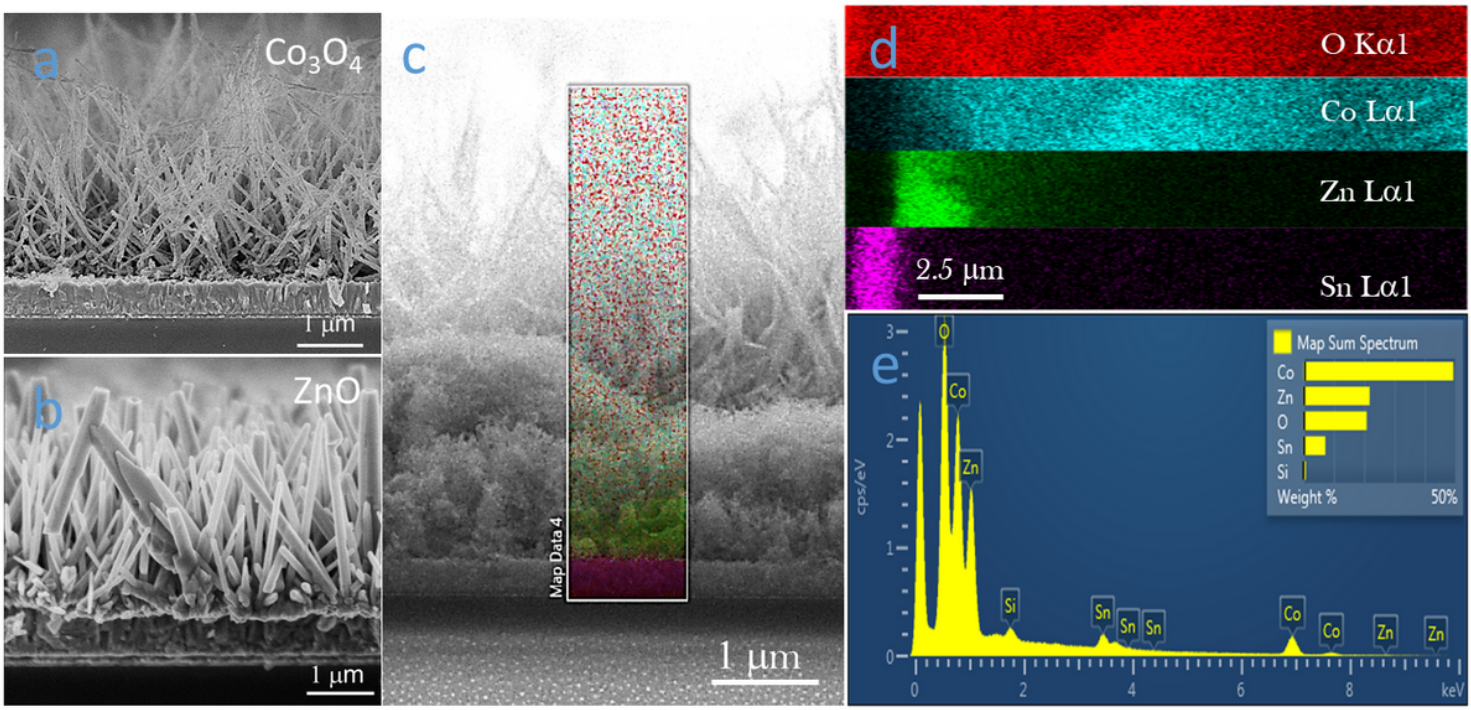

Figure 2

The cross-section SEM images of a) pure ZnO, b) pure Co3O4, and c) the ZnO covered with Co3O4 nanorods along with d) the elemental distribution in their heterostructures and a representative EDS spectrum (e).

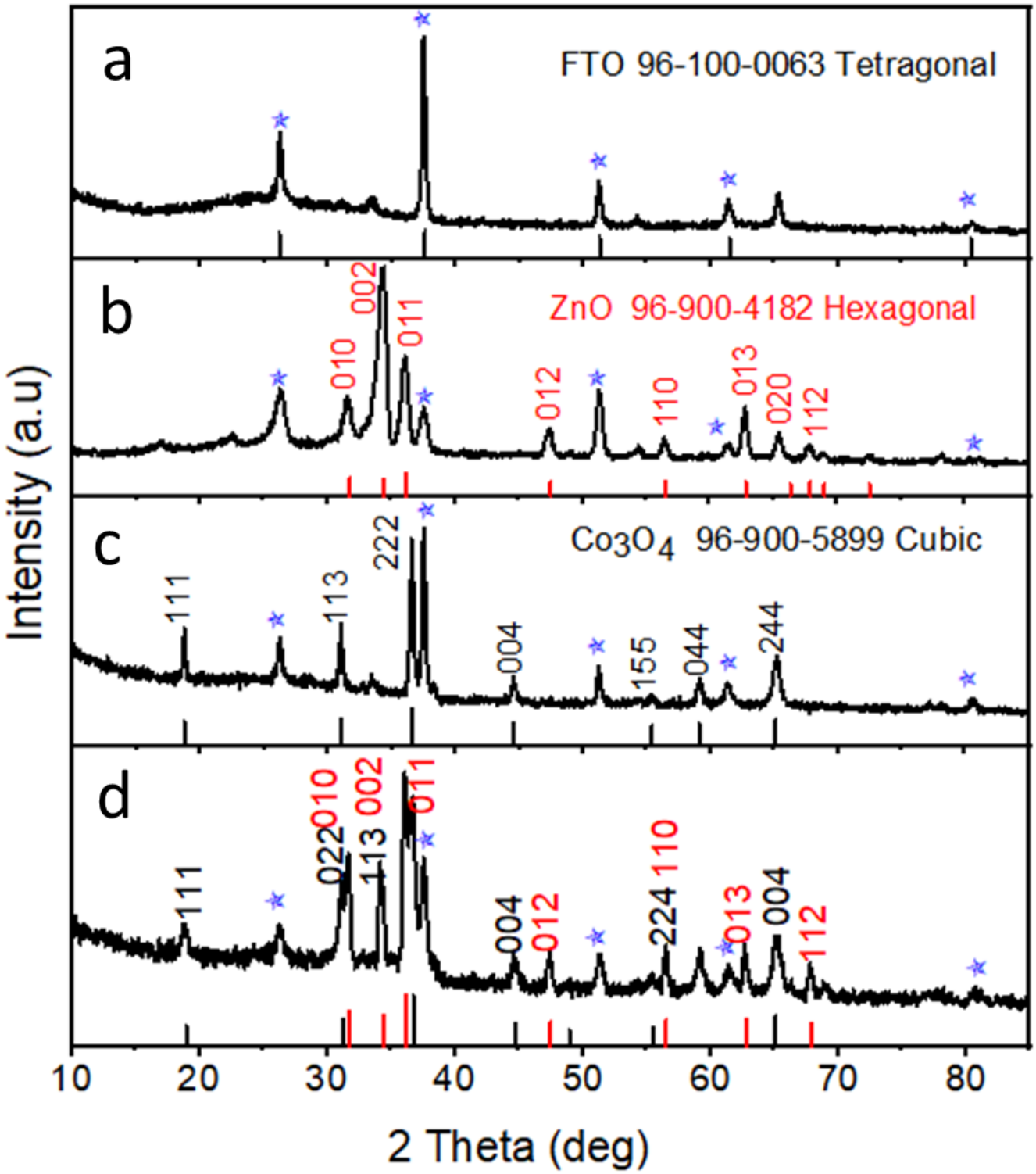

Figure 3

a. XRD of FTO, b. The XRD of pure ZnO nanorods, c. The XRD of Co3O4 d. The XRD of Co3O4 / ZnO nanorods by low temperature aqueous chemical growth method

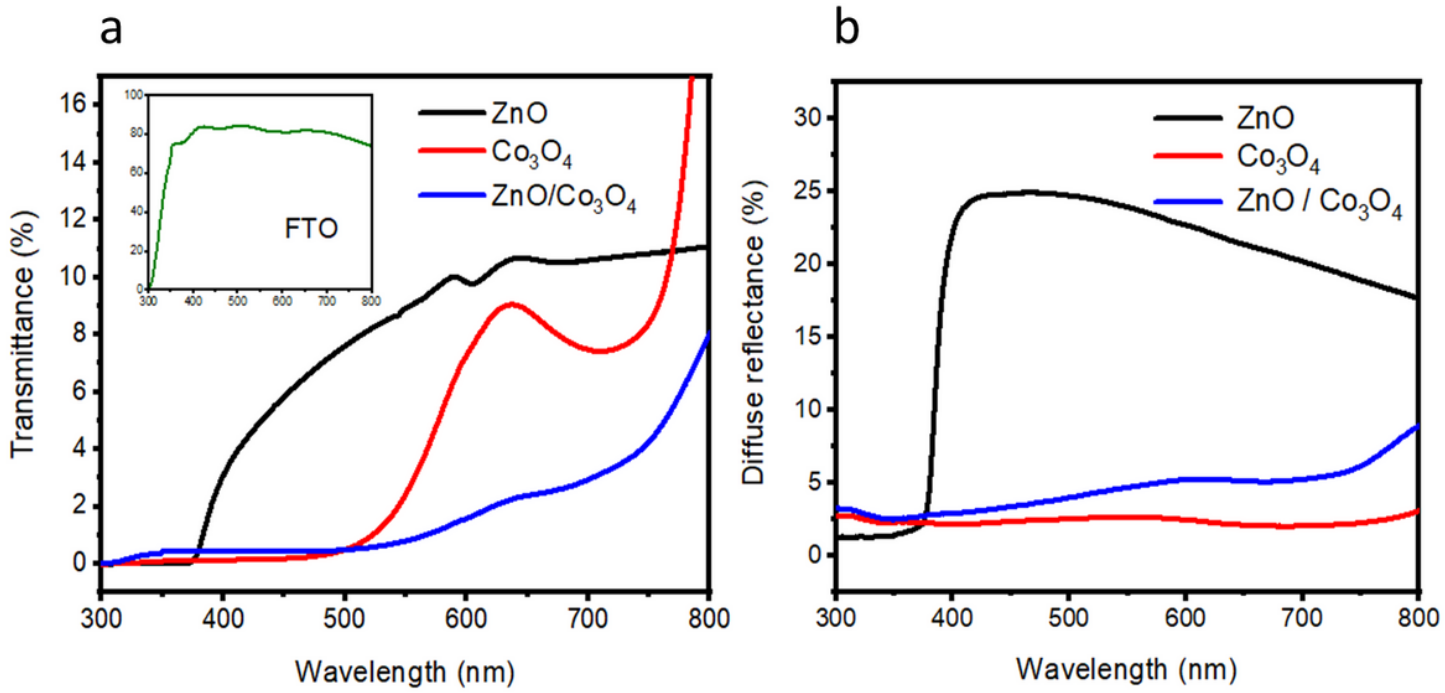

Figure 4

The optical transmittance and diffused reflectance of various materials used in the fabrication of Co3O4 decorated ZnO nanorods

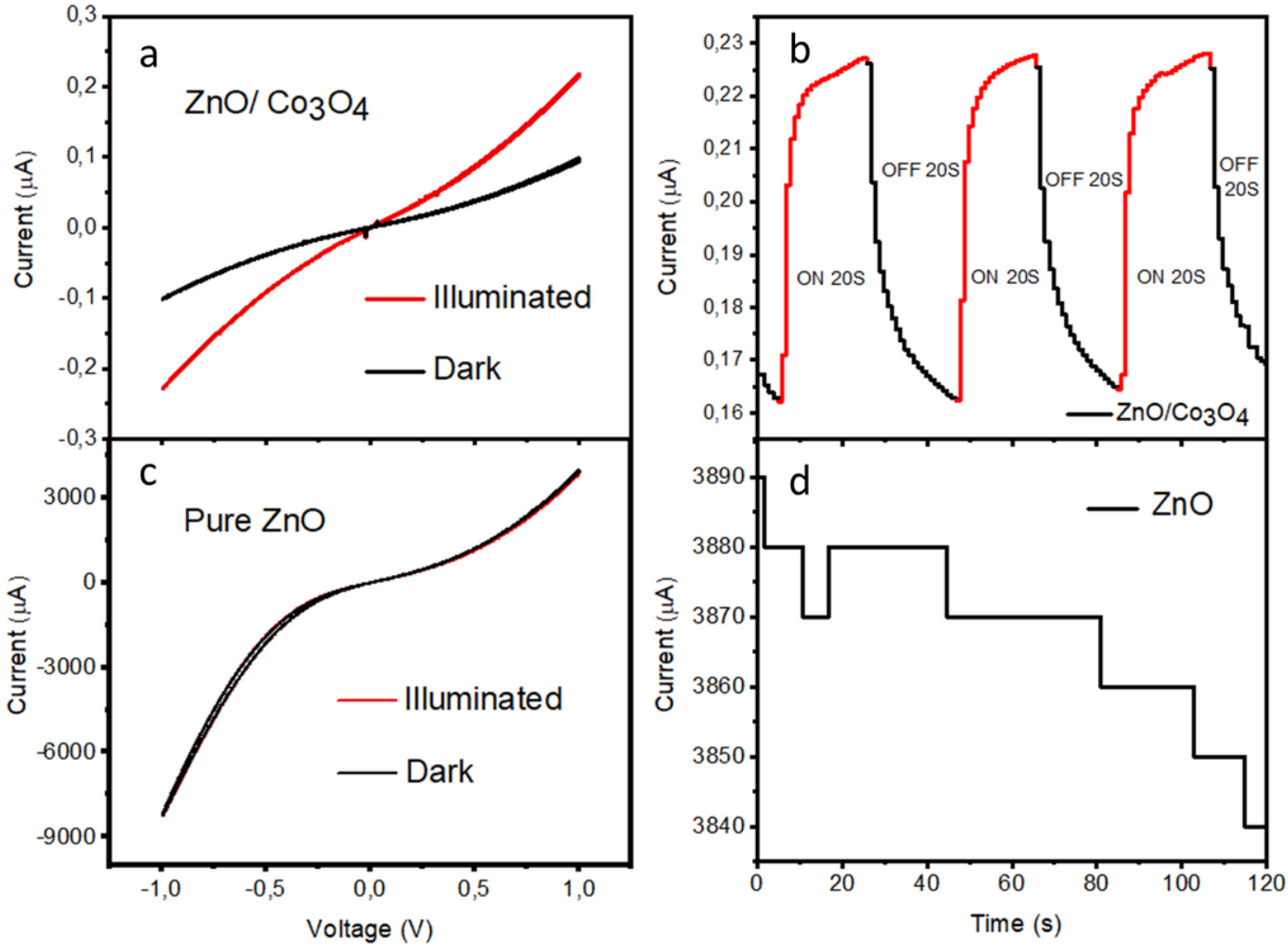

Figure 5

a. I-V characteristics of visible light photodetector, b. on/off light response of developed photosensor at bias voltage of 1.0 V, c. I-V curve of pure ZnO, d. on/off light response of pure ZnO.